# Continued-fraction analysis of dressed systems: Application to periodically driven optical lattices

Thomas Zanon-Willette,[1,2,*] Emeric de Clercq,[3] and Ennio Arimondo[4]

[1]*UPMC Université de Paris 06, UMR 7092, LPMAA, 4 place Jussieu, case 76, 75005 Paris, France*
[2]*CNRS, UMR 7092, LPMAA, 4 place Jussieu, case 76, 75005 Paris, France*
[3]*LNE-SYRTE, Observatoire de Paris, CNRS, UPMC, 61 avenue de l'Observatoire, 75014 Paris, France*
[4]*Dipartimento di Fisica "E. Fermi", Università di Pisa, Largo B. Pontecorvo 3, 56122 Pisa, Italy*

Radio-frequency quantum engineering of spins is based on the dressing by a nonresonant electromagnetic field. Radio-frequency dressing occurs also for the motion of particles, electrons, or ultracold atoms, within a periodic spatial potential. The dressing, producing a renormalization and also a freeze of the system energy, is described by different approaches: dressed atom, magnetic resonance semiclassical treatment, and continued-fraction solution of the Schrödinger equation. A comparison between these solutions points out that the semiclassical treatment, to be denoted as the *S* solution, represents the most convenient tool to evaluate the tunneling renormalization of ultracold atoms.

PACS number(s): 37.10.Jk, 32.80.Qk, 31.15.xg

## I. INTRODUCTION

The analysis of a system with few degrees of freedom, an electron or an atom, interacting with a large system, photons or phonons, relies often on a renormalization approach, where the parameters of the initial system are modified by the interaction. Examples of this approach are the effective mass for the electron motion in a semiconductor, or the extensive renormalization in quantum electrodynamics. Another example is the dressed atom introduced by Cohen-Tannoudji in order to describe the modification of a two-level atomic magnetic response by an applied radio-frequency (rf) field in the absence of decoherence processes [1]. For a nonresonant rf driving at a high frequency Cohen-Tannoudji and Haroche [2] derived a renormalization of the atomic level splitting dependent on the amplitude of the rf field and described by a zeroth-order ordinary Bessel function. That modification producing a magnetic "freezing" of the two-level response (i.e., a nonmagnetic system) was examined for atoms in [3–6], for a Bose-Einstein condensate of chromium in [7], for an artificial atom in [8], and recently proposed for improving the precision of optical clocks [9].

The same renormalization and freezing of the system properties under the application of a time-dependent modulation was applied to a variety of processes, all characterized by weak decoherence processes. We mention here the dynamical localization describing the renormalized motion of a charged particle within a periodic potential under a time-modulated force [10] and the coherent destruction of tunneling for a double-well potential with a periodic driving, with a complete localization of a wave packet in one well for specific values of the driving force [11]. For the motion of ultracold degenerated atomic gases within a shaken optical lattice, the tunneling atomic evolution is renormalized under the application of a time-modulated force, as proposed in [11–16] and tested experimentally in [17–22] within the framework of quantum simulation of solid-state physics. The renormalization of an

optical lattice potential acting on cold atoms in a regime of classical diffusion and transport was investigated in [23].

The target of the present work is to characterize the renormalization and freezing for a wide parameter range. The starting point is the continued-fraction solution for the two-level atomic magnetic response to an applied rf field, as typical of the nuclear magnetic resonance for a one-half spin. The regime of strong perturbation was investigated by several authors [24–28], in the presence or absence of decoherence. Their solution was expressed in terms of infinite continued fractions. The present work investigates the renormalization process through the continued-fraction approach. That treatment allows us to explore numerically the shaken-lattice renormalization for all parameter ranges, and in particular for explored experimental conditions. The numerical complexity of the continued-fraction solution, and its slow convergence in the regime of experimental interest, brought us to consider carefully the corrections to the zero-order Bessel function derived for the dressed-atom problem mainly through a semiclassical treatment [29–32], and later recovered through renormalization group techniques [33]. On the basis of the analogy between the renormalization of the magnetic resonance energy and of the atomic tunneling in optical lattice, we focus our analysis on the high-frequency regime realized for a rf modulation at a very large frequency. Then we explore the corrections when this limiting condition is not precisely satisfied. The low-frequency regime covered by the treatments of Refs. [10,14,16,34] is not examined here.

Section II presents different systems where the renormalization of the interaction strength has been investigated: magnetic resonance, motion in a periodic potential, and tunnel coupling in a periodic potential. This section reports also the standard result of the renormalization process given by the zero-order Bessel function, valid under appropriate operating conditions. Section III reports the solution for the temporal evolution of the wave function in the magnetic resonance case. Section IV derives the renormalization through the continued-fraction approach, valid for all operating conditions, and also through a semiclassical treatment refining the Bessel-function result. Section V reports numerical results determining the limiting validity of the usual zero-order Bessel correction, and derives

---

*thomas.zanon@upmc.fr

the renormalization for a large set of parameters. A conclusion completes our work.

## II. DRESSED SYSTEMS

### A. Magnetic resonance

(a) *Semiclassical approach.* For a spin-1/2 system interacting with a static magnetic field along the $z$ axis and driven by an oscillating rf field along the $x$ axis, the semiclassical Hamiltonian $H_{\rm sc}$ is

$$H_{\rm sc} = \frac{\hbar\omega_0}{2}\sigma_z + \frac{\hbar\Omega}{2}\cos(\omega t)\sigma_x, \qquad (1)$$

where $\sigma_{x,z}$ are the Pauli matrices, $\hbar\omega_0$ the energy splitting between the magnetic levels, and $\Omega$ the Rabi frequency proportional to the rf field amplitude.

By writing the atomic wave function $|\psi\rangle$ written as a superposition of the $|\pm\rangle$ atomic eigenfunctions

$$|\psi(t)\rangle = \sum_{m=\pm} C_{\rm m}(t)|m\rangle, \qquad (2)$$

the Schrödinger equation leads to the following temporal evolution for the $C_{\rm m}$ coefficients:

$$i\dot{C}_+ = \frac{\omega_0}{2}C_+ + \frac{\Omega}{2}\cos(\omega t)\,C_-,$$
$$i\dot{C}_- = -\frac{\omega_0}{2}C_- + \frac{\Omega}{2}\cos(\omega t)\,C_+. \qquad (3)$$

In the $\omega_0 \to 0$ limit, and for $C_+(t=0)=1$ as initial condition, these equations have solution

$$|\psi(t)\rangle = \cos\left[\frac{\Omega}{2\omega}\sin(\omega t)\right]|+\rangle - i\sin\left[\frac{\Omega}{2\omega}\sin(\omega t)\right]|-\rangle. \qquad (4)$$

As in [7,27] the result of calculating the $\sigma_z$ time-averaged mean value over $|\psi\rangle$ may be expressed through the following renormalized eigenvalues of the $H_{\rm sc}$ Hamiltonian:

$$E_\pm^{\rm ren} = \pm\frac{\hbar\omega_0}{2}\mathcal{J}_0\left(\frac{\Omega}{\omega}\right). \qquad (5)$$

The introduction of a renormalization coefficient $R$ defined by the ratio between renormalized and original eigenvalues leads to

$$\mathcal{R} = \frac{E_\pm^{\rm ren}}{\pm\frac{1}{2}\hbar\omega_0} = \mathcal{J}_0\left(\frac{\Omega}{\omega}\right), \qquad (6)$$

depending on the zero-order ordinary Bessel function $\mathcal{J}_0$. Thus the applied sinusoidal magnetic interaction renormalizes the atomic coupling to the static magnetic field, with a reduction by the factor $\mathcal{J}_0(\frac{\Omega}{\omega})$. The effective magnetic energy is frozen whenever $\Omega/\omega$ is a zero root of the $\mathcal{J}_0$ Bessel function, as observed in the experiments of Refs. [3–5,7]. The magnetic resonance renormalization was explored by Ref. [6] in the $\omega < \omega_0$ low-frequency regime, where the present approach is not valid.

(b) *Quantized approach.* Introducing a quantum description of the rf field, with operator $a^\dagger$ and $a$ for the creation and annihilation of one radio-frequency photon, the dressed-atom

Hamiltonian $H_{\rm da}$ of the above configuration is [35]

$$H_{\rm da} = \hbar\omega a^\dagger a + \frac{\hbar\Omega}{\sqrt{2\bar{n}}}(a + a^\dagger)\sigma_x + \frac{\hbar\omega_0}{2}\sigma_z, \qquad (7)$$

where $\bar{n}$ represents the mean number of photons applied to the atoms.

For the high-frequency case $\omega \gg \omega_0$ the last term in $H_{\rm da}$ may be neglected and its eigenstates easily determined. Then a perturbation treatment for the $\sigma_z$ term of that Hamiltonian leads to Eq. (5) for describing the interaction with the static field [35]. The previous renormalization result is obtained also through this approach.

Notice that the dressed-atom approach, and also the semiclassical approach of [32], demonstrated that the $\mathcal{J}_0$ renormalization is valid for whatever spin value and equally spaced Zeeman levels.

### B. Dynamic localization

Dynamic localization was introduced by Dunlap and Kenkre [10] for the motion of an electron on a discrete one-dimensional periodic lattice with spacing $d_L$ in the presence of an oscillating force. It is based on exact calculations for the particle motion. A single-particle basis useful for describing the electron tunneling among the discrete lattice sites is provided by the $j$th Wannier function centered on the $j$ lattice site of the periodic potential [36]. In a given energy band the Hamiltonian for free motion on the periodic lattice is determined by tunneling matrix elements, which in general connect arbitrarily spaced lattice sites. However, because the hopping amplitude decreases rapidly with the distance, the tunneling Hamiltonian may be well approximated by including only the $\hbar J$ tunneling energy hopping between neighboring lattice sites. Under this hypothesis, the Hamiltonian for the electron on the linear lattice with an applied periodic force $F\cos(\omega t)$ is [10,37]

$$H_{dl} = \hbar J \sum_m (|j\rangle\langle j+1| + |j+1\rangle\langle j|)$$
$$+ \hbar K \cos(\omega t) \sum_j j|j\rangle\langle j|. \qquad (8)$$

Here $\hbar K = Fd_L$ is the time-modulated energy difference between neighboring lattice sites. Dynamic localization entails a suppression of the particle transport with the particle position oscillating in time and returning periodically to its original value. It is associated with particle motion on an infinite lattice and does not impose conditions on the frequency driving. Our focus based on the analogy with magnetic resonance is on the high-frequency driving and on a lattice with a site finite number.

For the case of two lattice sites ($j = -1/2, 1/2$), introducing the Pauli operators as $\sigma_z = |1/2\rangle\langle 1/2| - |-1/2\rangle\langle -1/2|$ and so on, the above Hamiltonian becomes [38]

$$H_{dl} = \hbar J \sigma_x + \frac{\hbar\Omega}{2}\cos(\omega t)\,\sigma_z, \qquad (9)$$

where we have introduced $\Omega = K$ in order to emphasize the equivalence of this Hamiltonian with that of Eq. (1) apart from a change of the quantization axes and the $J \equiv \omega_0/2$ parameter correspondence. Therefore the dressed-atom renormalization

TABLE I. Values of the shaken-lattice experimental parameters, $J$ equivalent to $\omega_0/2$, $\omega$, $\Omega = K/\hbar$, measured in units of the recoil frequency $\omega_{\rm rec}/2\pi$ of the investigated atom. The last column reports the $\omega_0/\omega$ ratio.

| Ref. | $J \equiv \omega_0/2$ | $\omega$ | $\Omega$ | $\omega_0/\omega$ |
|------|------|------|------|------|
| [17] | 0.02–0.08 | 0.15–0.9 | 0–6 | 0.04–1.0 |
| [18] | 0.19 | 0.8–4 | 0–1.2 | 0.09–0.47 |
| [19] | 0.004 | 1.9 | 0–3 | 0.004 |
| [20] | 0.002 | 0.9 | 0–5 | 0.004 |
| [22] | 0.02 | 0.9 | 0–9 | 0.04 |

applies also to this system, leading to a renormalized tunneling rate,

$$J_{\rm eff} = \mathcal{R}J. \qquad (10)$$

Once again the system response is frozen whenever $\Omega/\omega = K/(\hbar\omega)$ is a root of the $\mathcal{J}_0$ Bessel function. The applied sinusoidal force produces a dynamic localization of the particle.

For a spin larger than one-half and more than two lattice sites, the Hamiltonian assumes a form equivalent to that of Eq. (9), except for the angular momentum. Thus the magnetic resonance analogy confirms the $\mathcal{R}$ renormalization also for an arbitrary number of lattice sites.

### C. Shaken optical lattice

In a 1D optical lattice ultracold atoms are confined within the potential minima created by a single laser standing wave with $d_L$ spacing [39,40]. The Hamiltonian for atomic motion on the periodic lattice is determined by tunneling matrix typically including only the $J$ hopping between neighboring lattice sites.

A periodic force $F\cos(\omega t)$ (to be referred as lattice shake) drives the atoms inside the optical lattice. Using the $j$th Wannier function centered on the $j$ lattice site, the Hamiltonian of Eq. (8) describes also the motion of the ultracold atoms within the optical lattice, with $K = \Omega$ again the shaking energy difference between neighboring sites of the linear chain. Therefore the dynamic localization and the renormalization of the previous subsection applies also to the ultracold-atom shaken lattices [11–16], as tested in several experiments [17–22]. The parameters of the Hamiltonian of Eq. (9) investigated in those experiments are reported in Table I. Notice that most experiments investigated the high-frequency regime, but large deviations from that regime also occurred. Reference [41] pointed out the difficulties in the precise measurement of the tunneling freeze from the ultracold-atom images.

### III. CONTINUED-FRACTION APPROACH

If a single-particle Hamiltonian is periodic in time, with period $T$, then the Floquet's theorem [42] states the existence of a set of distinguished solutions $|\psi_n(t)\rangle$ to the time-dependent Schrödinger equation. These Floquet states, analogous to the usual energy eigenstates of time-independent Hamiltonian operators [21,25,43], have the form

$$|\psi_n(t)\rangle = |u_n(t)\rangle \exp(-i\varepsilon_n t/\hbar), \qquad (11)$$

with time periodic functions $|u_n(t)\rangle = |u_n(t + T)\rangle$. The quantum number $n$ specifies the state. The quantities $\varepsilon_n$ are denoted quasienergies. By inserting Eq. (11) into the Schrödinger equation governed by the $H_{\rm sc}$ Hamiltonian, we deduce

$$\left(H_{\rm sc} - i\hbar\frac{\partial}{\partial t}\right)|u_n(t)\rangle = \varepsilon_n|u_n(t)\rangle, \qquad (12)$$

to be regarded as an eigenvalue equation for the Floquet quasienergies. The set of Floquet functions is complete in the Hilbert space on which acts the Hamiltonian. Hence, any solution $|\psi(t)\rangle$ to the Schrödinger equation admits an expansion in the $|u_n(t)\rangle$ basis.

If $|u_n(t)\rangle$ be a solution to the eigenvalue Eq. (12) with quasienergy $\varepsilon_n$, then $|u_n(t)\rangle e^{im\omega t}$ also is a $T$-periodic solution, with quasienergy $\varepsilon_n + m\hbar\omega$ $m$ being an arbitrary integer, where $\omega = 2\pi/T$. Therefore the quasienergy of a Floquet state is determined only up to an integer multiple of the $\hbar\omega$ photon energy. In accordance with the solid-state physics terminology, the quasienergy spectrum is said to consist of an infinite set of identical Brillouin zones of width $\hbar\omega$, covering the entire energy axis, each state placing one of its quasienergies in each zone.

The quasienergies may be determined by diagonalization of the Hamiltonian expressed in the Fourier space, as in [25], or equivalently diagonalizing the dressed-atom Hamiltonian as in [35]. We will make use of the continued-fraction solution of Refs. [24,27]. We apply the Fourier expansion to the $C_\pm$ coefficients of Eq. (2)

$$C_-(t) = e^{i\lambda t}\sum_{n=-\infty}^{n=+\infty} A_n e^{-in\omega t}, \quad C_+(t) = e^{i\lambda t}\sum_{n=-\infty}^{n=+\infty} B_n e^{-in\omega t}. \qquad (13)$$

Substituting these expansions into Eq. (3) and equating the same order Fourier components, one obtains

$$\left(\lambda - \frac{\omega_0}{2} - n\omega\right)A_n = -\frac{\Omega}{4}B_{n-1} - \frac{\Omega}{4}B_{n+1}, \qquad (14a)$$

$$\left(\lambda + \frac{\omega_0}{2} - n\omega\right)B_n = -\frac{\Omega}{4}A_{n-1} - \frac{\Omega}{4}A_{n+1}. \qquad (14b)$$

These equations can be separated into a first set with all even $A$'s and odd $B$'s being zero,

$$\left(\tilde\lambda_+ - \frac{4\omega_0}{\Omega} - l\frac{4\omega}{\Omega}\right)A_l = -B_{l-1} - B_{l+1}, \qquad (15a)$$

$$\left(\tilde\lambda_+ - k\frac{4\omega}{\Omega}\right)B_k = -A_{k-1} - A_{k+1}, \qquad (15b)$$

and into a second one with all odd $A$'s and even $B$'s being zero,

$$\left(\tilde\lambda_- - k\frac{4\omega}{\Omega}\right)A_k = -B_{k-1} - B_{k+1}, \qquad (16a)$$

$$\left(\tilde\lambda_- + \frac{4\omega_0}{\Omega} - l\frac{4\omega}{\Omega}\right)B_l = -A_{l-1} - A_{l+1}. \qquad (16b)$$

Here we have $k$ even, $l$ odd, and we introduce

$$\tilde\lambda_+ = \frac{4}{\Omega}\left(\lambda + \frac{\omega_0}{2}\right),$$

$$\tilde\lambda_- = \frac{4}{\Omega}\left(\lambda - \frac{\omega_0}{2}\right). \qquad (17)$$

Equations (15) and (16) are independent and a complete solution is obtained by adding the solutions of these equations. Equation (16) may be rewritten as

$$x_j = -\frac{x_{j-1} + x_{j+1}}{D_j} \tag{18}$$

by imposing $x_j \equiv A_j$ for even $j$, $x_j \equiv B_j$ for odd $j$, with

$$D_j \equiv \tilde{\lambda}_- + 4\omega_0/\Omega - j4\omega/\Omega \quad \text{for odd } j, \tag{19a}$$

$$D_j \equiv \tilde{\lambda}_- - j4\omega/\Omega \quad \text{for even } j. \tag{19b}$$

The recurrence Eq. (18) has a continued-fraction solution [27, 44], with expression for $j > 0$

$$\frac{x_j}{x_{j-1}} = -\frac{1}{D_j - \dfrac{1}{D_{j+1} - \dfrac{1}{D_{j+2} - \frac{1}{\dots}}}} \tag{20}$$

and similar expression for a negative $j$. By replacing $x_1$ and $x_{-1}$ into Eq. (18) for $j = 0$, we obtain the continued-fraction solutions for $\tilde{\lambda}_+$ and $\tilde{\lambda}_-$, with

$$\tilde{\lambda}_- = \frac{1}{\tilde{\lambda}_- + \frac{4\omega_0}{\Omega}\left(1 - \frac{\omega}{\omega_0}\right) - \dfrac{1}{\tilde{\lambda}_- - \frac{8\omega}{\Omega} - \frac{1}{\tilde{\lambda}_- + \frac{4\omega_0}{\Omega}\left(1 - 3\frac{4\omega}{\Omega}\right) - \frac{1}{\dots}}}}$$

$$+ \frac{1}{\tilde{\lambda}_- + \frac{4\omega_0}{\Omega}\left(1 + \frac{\omega}{\omega_0}\right) - \dfrac{1}{\tilde{\lambda}_- + \frac{8\omega}{\Omega} - \frac{1}{\tilde{\lambda}_- + \frac{4\omega_0}{\Omega}\left(1 + 3\frac{4\omega}{\Omega}\right) - \frac{1}{\dots}}}} \tag{21}$$

and

$$\tilde{\lambda}_+ = -\tilde{\lambda}_-. \tag{22}$$

All Floquet quasienergies are given by

$$\varepsilon_{\pm,n} = -\hbar\lambda = \hbar\left(\pm\frac{\omega_0}{2} - \frac{\Omega}{4}\tilde{\lambda}_\pm\right) + n\hbar\omega. \tag{23}$$

The continued-fraction solution allows us to determine numerically the Floquet quasienergies with the required accuracy. Figure 1 reports the quasienergies within one Brillouin zone vs $\omega_0$ for different values of the $\Omega/\omega$ parameter. Those energy diagrams may be applied to analyze either magnetic resonance or dynamical localization or shaken optical lattices. The zero crossing of the energy represents magic values where the effective magnetic energy or quantum tunneling are frozen at values different from $\omega_0 = J = 0$.

## IV. RENORMALIZATION VS $\omega_0$ VALUE

The energy renormalization, to be investigated on the basis of different theoretical approaches, will be concentrated on the magnetic resonance case, but the analysis of Sec. II has demonstrated that the substitution $J = \omega_0/2$ allows us to apply our results also to the shaken optical lattices.

(a) $\mathcal{J}_0$ *solution.* The two-level energy splitting at $\omega \gg \omega_0$ derived in Eq. (5) by the magnetic resonance treatment leads to the $\mathcal{R}$ renormalization given by $\mathcal{J}_0$ Bessel function of Eq. (6). The $\mathcal{J}_0$ renormalization approximation corresponds to the following quasienergies:

$$\frac{\varepsilon_{\pm,n}}{\hbar} = \pm\frac{\omega_0}{2}\mathcal{J}_0\left(\frac{\Omega}{\omega}\right) + n\omega. \tag{24}$$
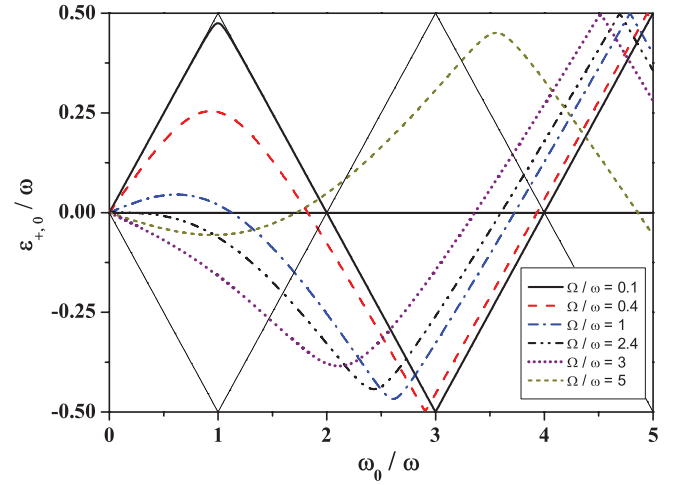


FIG. 1. (Color online) Central Brillouin zone of the quasienergy $\varepsilon_{+,0}$ vs $\omega_0$, both measured in $\omega$ units, for different values of $\Omega/\omega$, between 0 and 5. The quasienergy $\varepsilon_{-,0}$ is the opposite of $\varepsilon_{+,0}$. Quasienergies calculated by truncating the continued fraction to seven terms. Freezing occurs when the quasienergy is equal to zero at values different from $\omega_0 = 0$. For $\Omega/\omega = 2.4$ close to the $\mathcal{J}_0$ Bessel function first zero, owing to the quasienergy flatness at $\omega_0 \approx 0$ a nearly perfect freezing is reached in a large range of low $\omega_0$ values.

This solution predicts a freezing for whatever $\omega_0$ at the $\Omega/\omega$ values corresponding to the zeros of the $\mathcal{J}_0$ Bessel function, but its validity is limited to $\omega_0 \approx 0$.

(b) *S-corrected solution.* On the basis of a magnetic resonance semiclassical treatment, Refs. [30,32] derived an $\omega_0$-dependent correction to the $\mathcal{J}_0$ renormalization. That correction leads to the following quasienergies and renormalization:

$$\frac{\varepsilon_{\pm,n}}{\hbar} = \pm\frac{\omega_0}{2}\left[\mathcal{J}_0\left(\frac{\Omega}{\omega}\right) - \left(\frac{\omega_0}{\omega}\right)^2 S\left(\frac{\Omega}{\omega}\right)\right] + n\omega, \tag{25}$$

$$\mathcal{R} = \mathcal{J}_0\left(\frac{\Omega}{\omega}\right) - \left(\frac{\omega_0}{\omega}\right)^2 S\left(\frac{\Omega}{\omega}\right). \tag{26}$$

Here $S(x)$ is a product of $\mathcal{J}_n$ ordinary Bessel functions well approximated by the following expression [31]:

$$S(x) = \frac{16}{2025x^4}\left[\alpha(x)\mathcal{J}_2(x) + \beta(x)\mathcal{J}_4(x) - \gamma(x)\mathcal{J}_6(x)\right], \tag{27}$$

where $\alpha(x) = 75(5 - x^2/4)x^2$, $\beta(x) = 6(408 - 74x^2 - 23x^4/16)$, and $\gamma(x) = 145x^2\left(3 - x^2/2\right)/49$. Within the following section this solution will be used for calculations around the first and second zeros of the zeroth order Bessel function, and the validity limits for the $\omega_0/\omega$ application range will be discussed there.

(c) *Continued fraction.* A general approach to derive the $\mathcal{R}$ renormalization coefficient is based on the Floquet quasienergies derived in the previous section, leading to

$$\mathcal{R} = \frac{\varepsilon_{+,0}}{\hbar\omega_0/2}. \tag{28}$$

This equation allows a numerical determination of $\mathcal{R}$ without restricting to the low $\omega_0$ values where the $\mathcal{J}_0$ approximation
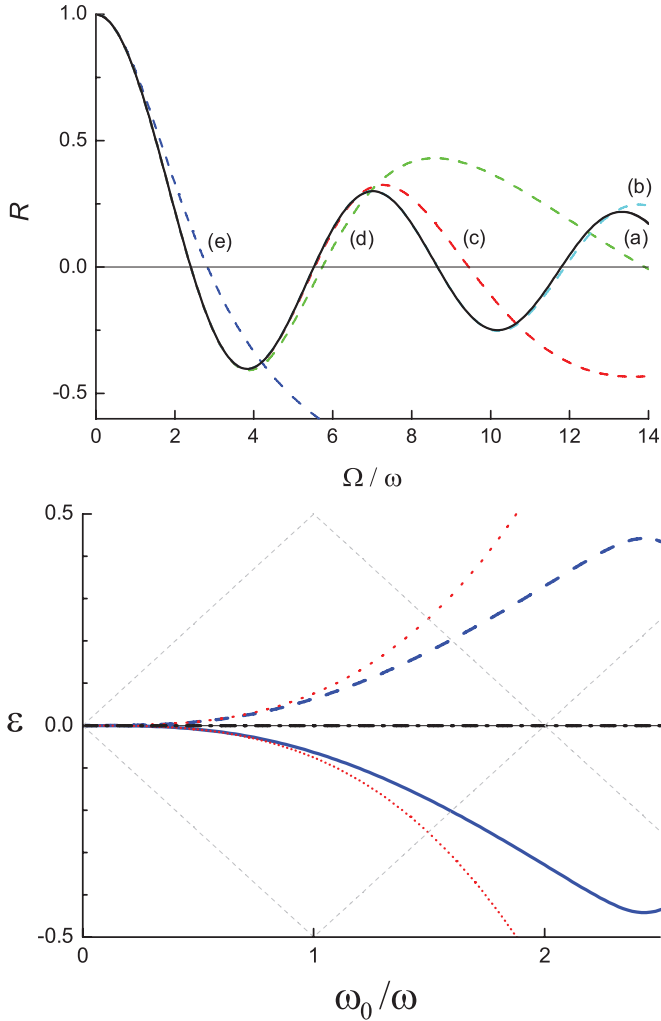
FIG. 3. (Color online) In (a) renormalization coefficient $\mathcal{R}$ and in (b) effective tunneling $\mathcal{J}_{\mathrm{eff}}$ vs $\Omega/\omega$ ratio for different values of $J/\omega$. Continuous blue lines for $J/\omega = 0.02$, dashed green lines for $J/\omega = 0.2$, and dotted red lines for $J/\omega = 0.4$.

FIG. 2. (Color online) On the top $\mathcal{R}$ vs $\Omega/\omega$ calculated at $\omega_0/\omega = 0.1$ on the basis of different approximations: (a) from the continued fraction containing terms up to 9 terms, the $\mathcal{J}_0$ solution of Eq. (5), and the $S$-corrected one of Eq. (26); (b), (c), (d) and (e) from the continued fraction limited to seven, four, three, and one terms, respectively. On the bottom quasienergies $\varepsilon_{+,0}$ (continuous lines) and $\varepsilon_{-,0}$ (dashed lines) vs $\omega_0$ at $\Omega/\omega = 2.405$. Thicker blue lines calculated on the basis of the four terms continued fraction; thinner red lines on the $S$-corrected solution. The central black horizontal dot-dashed line based on Eq. (24). Diagonal lines for the $\omega_0 \to 0$ quasienergies.

(without or with the $S$ function) is valid. The quasienergy can be derived either from the continued-fraction solution of Eq. (20), truncated to a finite number $j$ of terms, or from a diagonalization of the system of Eqs. (18) truncated to a finite number of equations with $2j + 1$ terms. The Hamiltonian diagonalization approach was applied in Ref. [6] for the renormalization calculations in both the low-frequency and high-frequency regimes.

## V. NUMERICAL RESULTS

The $\mathcal{R}$ renormalization coefficient is a complex function of the system parameters $\omega_0/\omega$ and $\Omega/\omega$, and the previous section approaches may be used for numerical analyses at different parameter values. Figure 2(a) reports the $R$ results at $\omega_0/\omega =$
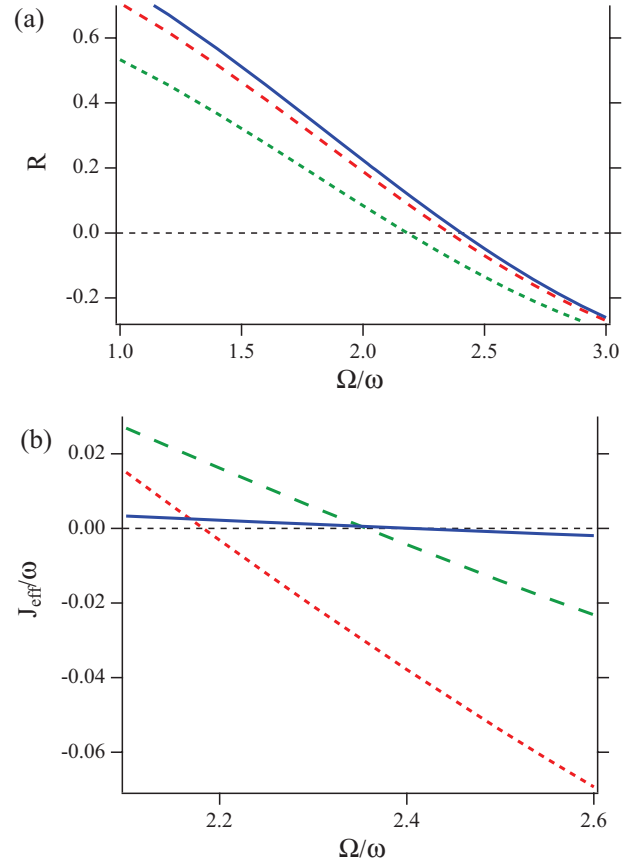
$2J/\omega = 0.1$ vs $\Omega/\omega$, obtained using Eq. (28) linking that coefficient to the Floquet quasienergies. For the quasienergies determined from the continued-fraction solution, and also from the diagonalization of the system of Eqs. (18), the results of Fig. 2(a) show a slow convergence at low $\omega_0$ values, as already pointed out by Autler and Townes [24], the number of required terms in the continued fraction depending on the $\Omega/\omega$ value. In the $\omega_0, J \to 0$ limit $\mathcal{R}$ is well approximated by the $\mathcal{J}_0(\Omega/\omega)$ function, the $S$ correction vanishing there.

For the quasienergies' dependence on $\omega_0$ at $\Omega/\omega = 2.405$, Fig. 2(b) compares the continued-fraction solution to the $\mathcal{J}_0$ solution and the $S$-corrected one. The $\mathcal{J}_0$ solution leads to a horizontal line close to the $x$ axis because $\Omega/\omega$ corresponds to the Bessel first zero, indicating that it approximates the quasienergies only for $\omega_0 \approx 0$. On the contrary the $S$-corrected solution approximates well the quasienergies for a large range of parameters, at least for $\omega_0/\omega$ up to 0.5 corresponding to $J/\omega$ up to 1.

For the shaken optical lattice experiments where the condition $\omega_0 = 2J \ll \omega$ is satisfied, as in most cases, the $\mathcal{J}_0$ solution is well appropriate for $\mathcal{R}$. At larger $J$ values, the $S$ function correction to $\mathcal{J}_0$ can be used for the full range of the parameters explored so far in experiments. Figure 3 reports an $S$-correction-based analysis of the shaken-lattice renormalization at increasing values of $J/\omega$. For $J/\omega = 0.4$ the correction to $\mathcal{R}$ shown in Fig. 3(a) is 10% smaller than
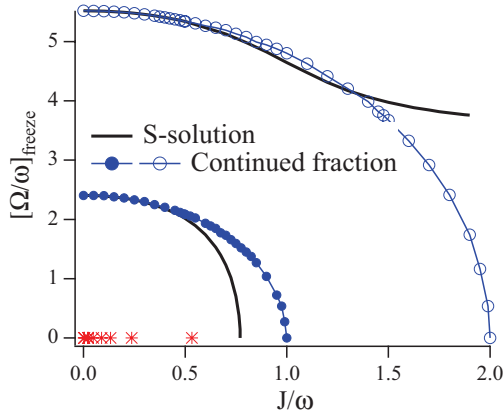
FIG. 4. (Color online) $[\Omega/\omega]_{\text{freeze}}$ values required to freeze the tunneling coefficient ($J_{\text{eff}} = 0$) as a function of the $J/\omega$ unperturbed tunneling coefficient. Continuous lines from the $S$-corrected expression and dots from the continued-fraction solution. Closed blue dots for the first zero crossing of the eigenenergies and open blue ones for the second zero crossing. The stars on the horizontal axis denote the $J/\omega$ values explored in the shaken optical lattice experiments.

the $J/\omega \approx 0$ value, but becomes larger increasing $J$. Because the most important quantity is the tunneling coefficient itself, Fig. 3(b) shows the $J_{\text{eff}} \approx 0$ dependence on $\Omega/\omega$ at increasing values of $J/\omega$. Notice that increasing $J/\omega$ the $J_{\text{eff}} = 0$ freezing configuration is reached at an $\Omega/\omega$ value lower than the Bessel first zero.

Figure 4 shows the $[\Omega/\omega]_{\text{freeze}}$ values required to produce a tunneling freeze for a given $J/\omega$ initial value. We plot the values associated with the first and second zero crossing of the eigenenergies, corresponding to the first and second zero of the Bessel function within the $\mathcal{J}_0$ solution. A comparison between the $S$-corrected solution and the continued-fraction solution is presented, confirming that for most shaken-lattice experiments performed so far, the $S$-corrected solution provides a simple and precise determination of the modified tunneling parameter. For a larger range of parameters the continued-fraction solution should be used. The data points at $\Omega/\omega \rightarrow 0$ correspond to the quasienergy crossings in absence of rf drive and do not have a physical meaning. Notice that freezing can be produced also applying $\omega$ values lower than $J$,

a regime that was not yet examined in the experiments. It may be noticed that the general dependence of the freezing value of Fig. 4 is similar, although not identical to the Bloch-Siegert shift dependence investigated in [1,2,24,25,27–32]. In fact for an applied oscillating field, as in the present magnetic resonance configuration, all the crossings and anticrossings of the energy levels are shifted towards lower $\omega_0$ values by increasing $\Omega$ [35]. The Bloch-Siegert shift of the magnetic resonance is associated with the position of the energy anticrossings, while the freezing point is associated with the zero crossing of the eigenenergies.

## VI. CONCLUSIONS

We have examined the energy renormalization of a two-level system usually associated with the dressed-atom approach, but also derivable from a semiclassical analysis of the magnetic resonance. The $S$ solution derived in Ref. [9] for the Zeeman freezing of optical clocks is here applied to the optical lattice experiments. Within that framework the standard zero-Bessel dependence on the amplitude of the electromagnetic field amplitude, valid only at zero magnetic field, was extended to derive a general dependence on the magnetic field amplitude. That result is important for the main target of the present work, to use the magnetic resonance results in order to perform an accurate analysis of the renormalization occurring for the atomic quantum tunneling between the minima of an optical lattice in the shaken lattice experiments. The magnetic resonance correction to the energy renormalization allows us to derive a very general formula for the tunneling renormalization in shaken optical lattices. The conditions for the complete cancellation of the tunneling rate are functions of the tunneling energy without shaking and of the modulation frequency. The precise determination of the tunneling under different driving conditions will lead to a better control in the quantum simulation experiments based on optical lattices.

## ACKNOWLEDGMENTS

[1] C. Cohen-Tannoudji, *Atoms in Electromagnetic Fields* (World Scientific, 1994). Several of his papers are in this book and all of them available at http://www.phys.ens.fr/~cct/.

[2] C. Cohen-Tannoudji and S. Haroche, C. R. Acad. Sci. Série B **262**, 268 (1968).

[3] S. Haroche, C. Cohen-Tannoudji, C. Audoin, and J. P. Schermann, Phys. Rev. Lett. **24**, 861 (1970).

[4] E. Muskat, D. Dubbers, and O. Schärpf, Phys. Rev. Lett. **58**, 2047 (1987).

[5] A. Esler, J. C. Peng, D. Chandler, D. Howell, S. K. Lamoreaux, C. Y. Liu, and J. R. Torgerson, Phys. Rev. C **76**, 051302(R) (2007).

[6] P.-H. Chu *et al.*, Phys. Rev. C **84**, 022501(R) (2011).

[7] Q. Beaufils, T. Zanon, R. Chicireanu, B. Laburthe-Tolra, E. Marechal, L. Vernac, J. C. Keller, and O. Gorceix, Phys. Rev. A **78**, 051603(R) (2008).

[8] J. Tuorila, M. Silveri, M. Sillanpää, E. Thuneberg, Y. Makhlin, and P. Hakonen, Phys. Rev. Lett. **105**, 257003 (2010).

[9] T. Zanon-Willette, E. de Clercq, and E. Arimondo, Phys. Rev. Lett. **109**, 223003 (2012).

[10] D. H. Dunlap and V. M. Kenkre, Phys. Rev. B **34**, 3625 (1986).

[11] F. Grossmann, T. Dittrich, P. Jung, and P. Hänggi, Phys. Rev. Lett. **67**, 516 (1991).

[12] A. Eckardt, C. Weiss, and M. Holthaus, Phys. Rev. Lett. **95**, 260404 (2005).

[13] C. E. Creffield and T. S. Monteiro, Phys. Rev. Lett. **96**, 210403 (2006).

[14] K. Kudo, T. Boness, and T. S. Monteiro, Phys. Rev. A **80**, 063409 (2009).

[15] A. Eckardt *et al.*, Europhys. Lett. **89**, 10010 (2010).

[16] K. Kudo and T. S. Monteiro, Phys. Rev. A **83**, 053627 (2011).

[17] H. Lignier, C. Sias, D. Ciampini, Y. Singh, A. Zenesini, O. Morsch, and E. Arimondo, Phys. Rev. Lett. **99**, 220403 (2007).

[18] E. Kierig, U. Schnorrberger, A. Schietinger, J. Tomkovic, and M. K. Oberthaler, Phys. Rev. Lett. **100**, 190405 (2008).

[19] A. Zenesini, H. Lignier, D. Ciampini, O. Morsch, and E. Arimondo, Phys. Rev. Lett. **102**, 100403 (2009).

[20] J. Struck, C. Ölschläger, R. Le Targat, P. Soltan-Panahi, A. Eckardt, M. Lewenstein, P. Windpassinger, and K. Sengstock, Science **333**, 996 (2011).

[21] E. Arimondo, D. Ciampini, A. Eckardt, M. Holthaus, and O. Morsch, Adv. At. Mol. Phys. **61**, 516 (2012).

[22] J. Struck, C. Olschlager, M. Weinberg, P. Hauke, J. Simonet, A. Eckardt, M. Lewenstein, K. Sengstock, and P. Windpassinger, Phys. Rev. Lett. **108**, 225304 (2012).

[23] A. Wickenbrock, P. C. Holz, N. A. Abdul Wahab, P. Phoonthong, D. Cubero, and F. Renzoni, Phys. Rev. Lett. **108**, 020603 (2012).

[24] S. H. Autler and C. H. Townes, Phys. Rev. **100**, 703 (1955).

[25] J. H. Shirley, Phys. Rev. **138**, B979 (1965).

[26] S. Morand and G. Théobald, C. R. Acad. Sci. Paris **269**, 1142 (1969).

[27] S. Stenholm, J. Phys. B **5**, 878 (1972); **5**, 890 (1972).

[28] S. Swain, Adv. At. Mol. Opt. Phys. **22**, 387 (1985).

[29] C. Cohen-Tannoudji, J. Dupont-Roc, and C. Fabre, J. Phys. B **6**, L218 (1973).

[30] P. Hannaford, D. T. Pegg, and G. W. Series, J. Phys. B **6**, L222 (1973).

[31] F. Ahmad and R. K. Bullough, J. Phys. B **7**, L275 (1974).

[32] G. W. Series, Phys. Rep. **43**, 1 (1977).

[33] M. Frasca, Phys. Rev. B **71**, 073301 (2005), and references therein.

[34] Y. Kayanuma and K. Saito, Phys. Rev. A **77**, 010101R (2008).

[35] C. Cohen-Tannoudji, in *Cargese Lectures in Physics*, Vol. 2, edited by M. Levy (Gordon and Breach, New York, 1968).

[36] N. Ashcroft and N. Mermin, *Solid State Physics* (Saunders College, Philadelphia, 1976).

[37] S. Raghavan, V. M. Kenkre, D. H. Dunlap, A. R. Bishop, and M. I. Salkola, Phys. Rev. A **54**, R1781 (1996).

[38] A. Eckardt, T. Jinasundera, C. Weiss, and M. Holthaus, Phys. Rev. Lett. **95**, 200401 (2005).

[39] I. Bloch, J. Phys. B **38**, S629 (2005).

[40] O. Morsch and M. Oberthaler, Rev. Mod. Phys. **78**, 179 (2006).

[41] C. E. Creffield, F. Sols, D. Ciampini, O. Morsch, and E. Arimondo, Phys. Rev. A **82**, 035601 (2010).

[42] G. Floquet, Ann. École Norm. Sup. **12**, 47 (1883).

[43] H. Sambe, Phys. Rev. A **7**, 2203 (1973).

[44] S. Stenholm and W. Lamb, Jr., Phys. Rev. **181**, 618 (1969).